ISJO Project Report

Timber Waste Recycling into Biochar and Carbonaceous Materials

Phase 1 – Feasibility Study

Project Number	2021/1
Prepared for	Illawarra Shoalhaven Joint Organisation, ISJO
Attention	Ms. Yvette Barrs Ms. Nicole Parsons
Prepared by	Dr. Rajkamal Balu Prof. Namita Roy Choudhury Chemical & Env. Engineering Discipline Prof. Usha Iyer-Raniga School of Property, Construction & Project Management **RMIT University**
Date of issue	25 November 2021
Distribution	Illawarra Shoalhaven Joint Organisation ISJO, NSW.

---

1. Executive summary

ISJO approached RMIT for a circular economy solution to deal with the problem of large amount of household and joinery timber waste that goes to landfill. A two-phase approach (Phase 1: Feasibility study, and Phase 2: Product development) for recycling timber waste into biochar and carbonaceous materials was proposed by RMIT Circular Economy Hub. Three waste samples obtained from different sources and conditions (details provided in section 2) were provided by ISJO. The Phase 1 study was performed at RMIT using pyrolysis (thermal degradation under inert atmosphere) as a recycling method for the conversion of the waste samples into biochar and carbonaceous materials, and the outcomes of the study are summarized in this report. Fixed-bed pyrolysis (under nitrogen) of the waste samples produced biochar, bio-oil, and syngas (largely comprising a mixture of hydrogen, methane, carbon monoxide and carbon dioxide). Physicochemical properties of the materials and gases evolved, i.e. (i) thermal degradation profile, composition, functional groups and organic content of as-received waste samples, (ii) functional groups, organic and inorganic content, structure and morphology, surface area and porosity of biochar obtained by pyrolysis, and (iii) gaseous products released during the pyrolysis process was analyzed using various experimental techniques (listed in section 3). The biochars exhibited high carbon, low ash and very low inorganic content, and poorly crystalline turbostratic carbon structure. The biochar obtained from household waste sample exhibited relatively higher surface area and micropore volume compared to joinery waste samples; where, the biochar obtained from rain unexposed waste samples exhibited relatively higher nitrogen content compared to rain exposed. The obtained biochars have great potential for energy and environmental applications. This report also provides information on some relevant current technologies that can be applied in pilot-scale pyrolysis, a brief market analysis and future recommendations for Phase 2 study.

2. Materials and methods

2.1. Details of waste samples received from ISJO

Number of samples	**:** 3 in total
Name of samples	**:** Household clean not exposed to rain, or simply Home-clean (HC) Household exposed to rain, or simply Home-rain exposed (HR) Joinery dust clean commercial, or simply Industrial-clean (IC)
Weight of samples	**:** Around 2 kg each
Form of samples	**:** Fine powder to fine chips

Figure 1: *Picture of as-received samples.*

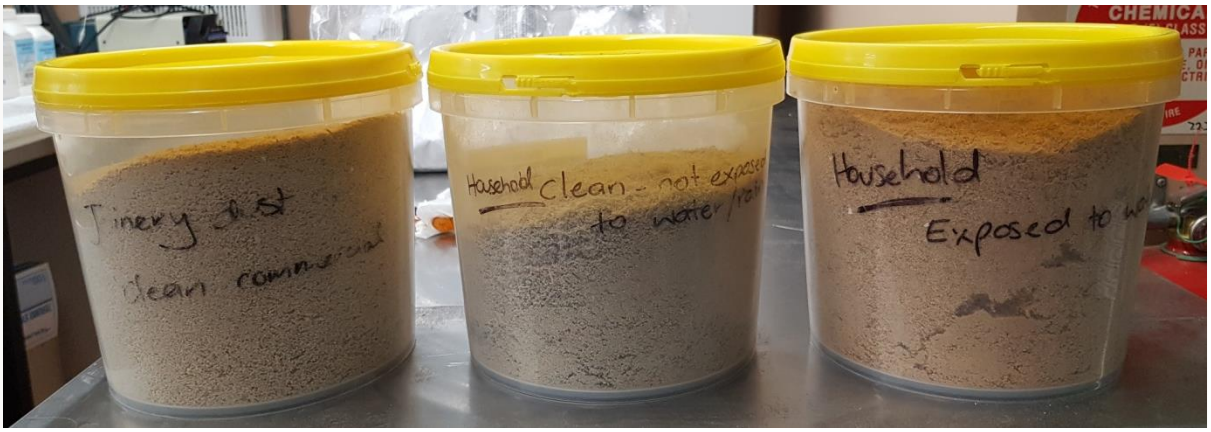

2.2. Sample characterization

Techniques used	Data obtained
Thermo gravimetric analysis (TGA)	Estimation of degradation temperature, composition and moisture content of as-received samples, yield of biochar from pyrolysis, and ash from combustion
Fourier transform infrared spectroscopy (FTIR)	Identification of functional groups in received samples, biochar and gaseous products from TGA pyrolysis
Gas chromatography–mass spectrometry (GC/MS)	Identification of gaseous products from TGA pyrolysis
Micro-Gas chromatography (miro-GC)	Identification of non-condensable gases from fixed-bed pyrolysis
Scanning electron microscopy (SEM)	Investigation of microstructure of biochar from TGA pyrolysis

X-ray diffraction (XRD)	Crystalline structure of biochar from TGA pyrolysis
Brunauer–Emmett–Teller (BET) analysis	Surface area and pore volume of biochar from TGA pyrolysis
CHNS elemental analysis	Quantification of C, H, N, S and O content in biochar from TGA pyrolysis
Inductively coupled plasma mass spectrometry (ICP-MS)	Quantification of inorganic elemental content in biochar from TGA pyrolysis

3. Experimental results

3.1. TGA

TGA of as-received timber waste samples was performed (in triplicates) using Netzch STA 449 F5 Jupiter$^{(R)}$ Instrument. Nitrogen (N_2) flow rate of 50 mL/min and a heating rate of 20 °C/min were used for analysis. TGA curves (Figure 2) and the respective first derivative weight loss curves (Figure 3) of waste samples are shown below. The as-received waste samples exhibited about 3.8% weight loss around 100 °C, which is attributed to the moisture present in the sample. The onset and offset of thermal degradation were observed around 200 °C and 500 °C, respectively for all three samples, which can be clearly observed in the derivative curves. A biochar yield of 23.1 ± 0.7, 21.4 ± 0.3 and 22.3 ± 0.6 wt% was measured for Home-clean (HC), Home-rain exposed (HR) and Industrial-clean (IC) samples, respectively. An ash content of 1.5 ± 0.4, 1.2 ± 0.4 and 1.6 ± 0.6 wt% was measured for HC, HR and IC samples, respectively by burning the biochar to 1000 °C in air atmosphere. The resin, hemicellulose, cellulose and lignin content of waste samples were estimated by deconvoluting the derivative curves (Figure 4) using their reported thermal degradation temperatures 230-240, 290-300, 350-360, 400-410 °C [1]. The calculated wt% of each component are given in Table 2.

Figure 2: *TGA curve of as-received samples.*

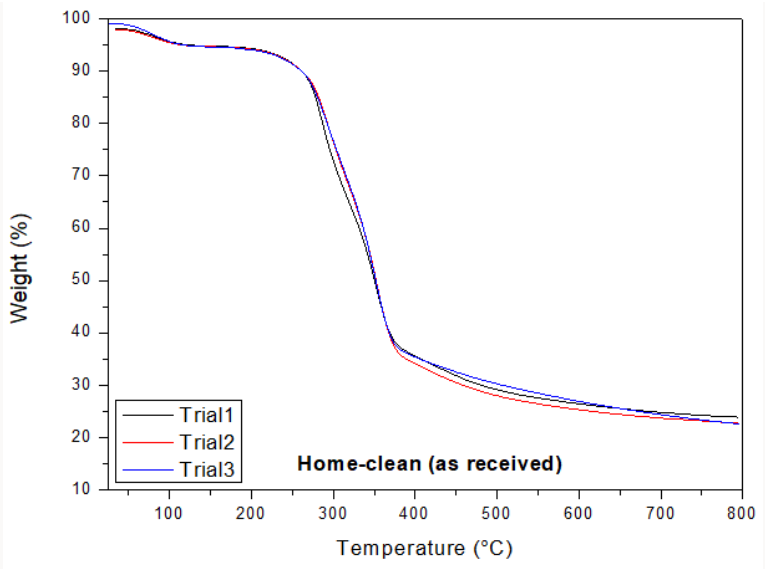

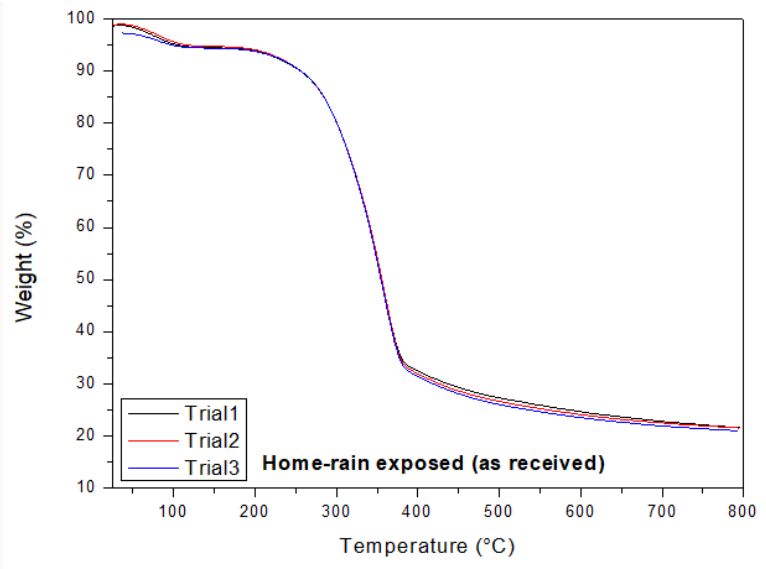

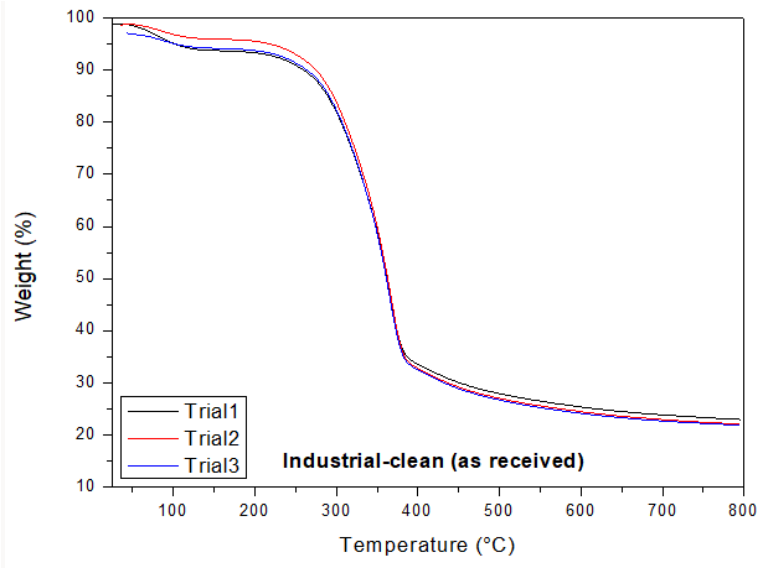

Figure 3: *TGA first derivative curve of as-received samples.*

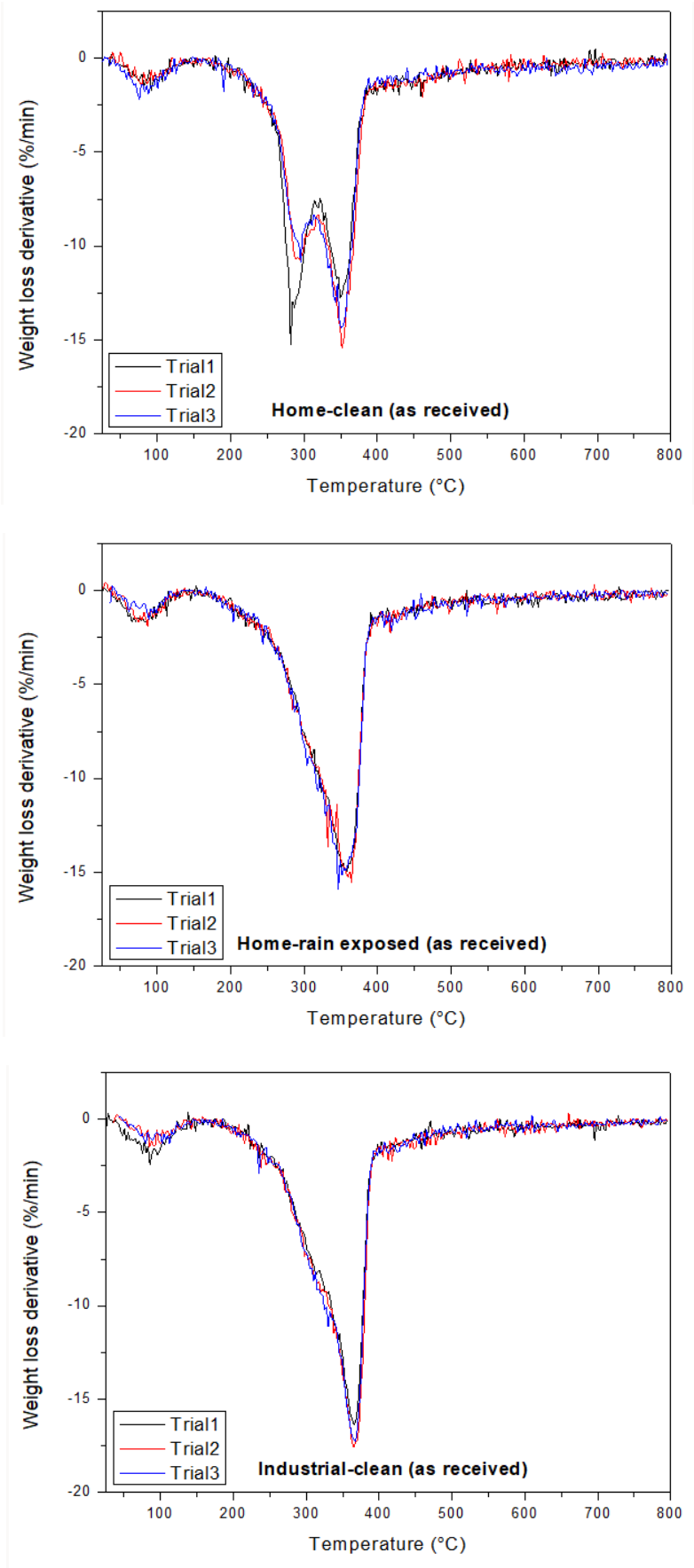

Figure 4: *Deconvolution of TGA first derivative curve of as-received samples.*

Home-clean (as-received)

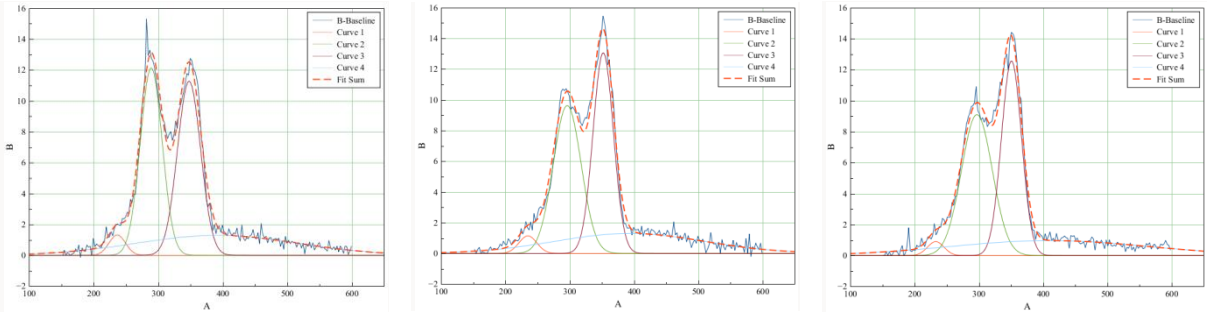

Home-rain exposed (as-received)

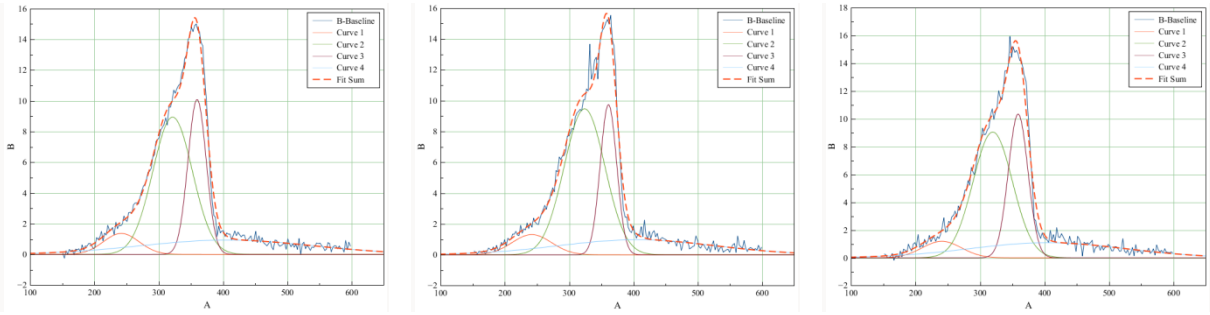

Industrial-clean (as-received)

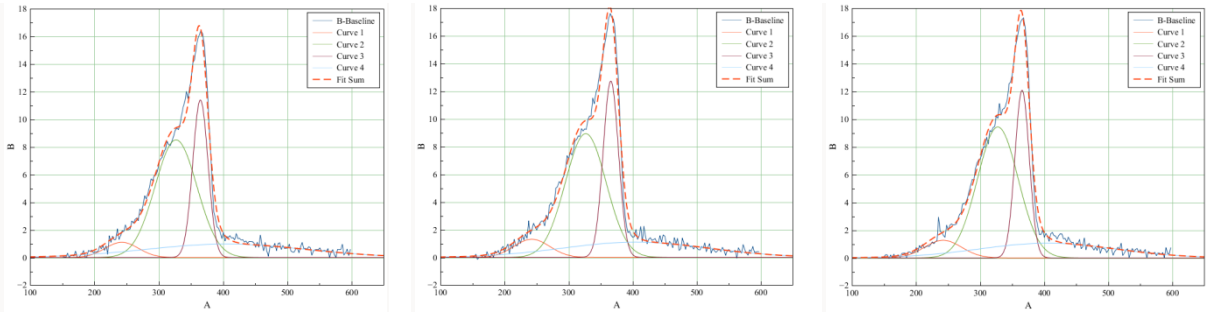

Table 2: *Composition of as-received samples obtained from TGA data deconvolution.*

Composition	Temperature (°C)	Home-clean (Wt.%)	Home-rain exposed (Wt.%)	Industrial-clean (Wt.%)
Moisture	90-110	3.6 ± 0.6	3.9 ± 0.8	3.6 ± 1.3
Resin	230-240	1.7 ± 0.3	4.6 ± 0.3	4.1 ± 0.5
Hemicellulose	290-300	24.8 ± 0.8	33.9 ± 2.0	34.5 ± 1.2
Cellulose	350-360	23.8 ± 0.7	16.9 ± 1.7	16.9 ± 1.0
Lignin	400-410	18.1 ± 0.7	15.0 ± 0.6	14.5 ± 0.8
Biochar	800	23.1 ± 0.7	21.4 ± 0.3	22.3 ± 0.6
Ash	1000 (air)	1.5 ± 0.4	1.2 ± 0.4	1.6 ± 0.6

3.2. FTIR

Functional group analysis of as-received timber waste samples and biochar from TGA pyrolysis was performed using PerkinElmer Frontier MIR/NIR FTIR spectrometer equipped with attenuated total reflection (ATR) accessory. FTIR spectra of waste samples (Figure 5) and biochars (Figure 6) are shown below, and their respective infrared band assignments obtained from literature [2] are given in Table 3. The biochars exhibited loss of O-H, C-H, C=O, H-O-H, CH, CH_2 and CH_3 functional groups.

Figure 5: *FTIR spectra of as-received samples.*

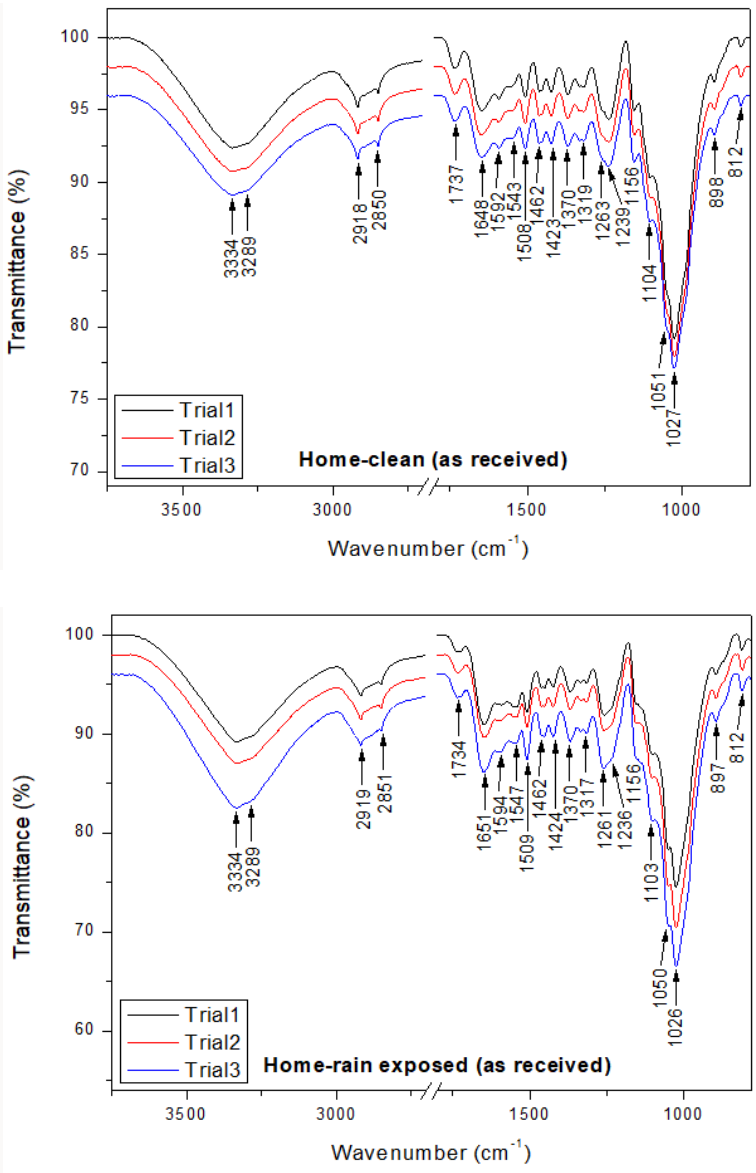

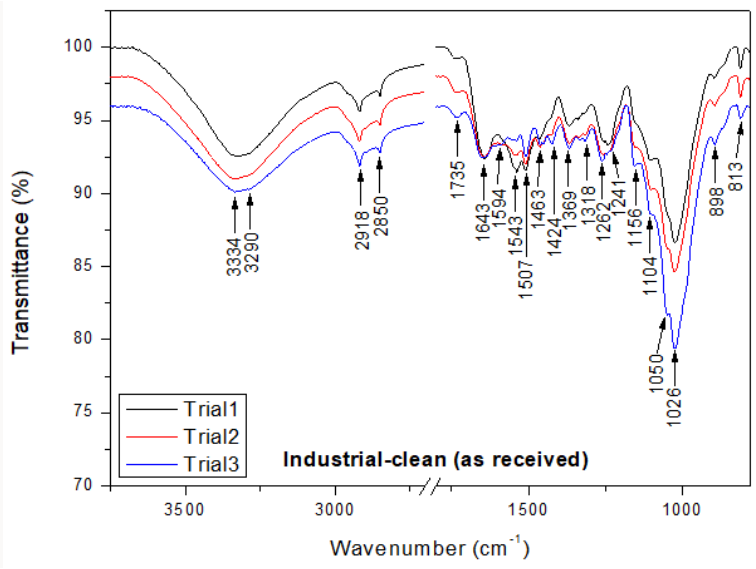

Figure 6: *FTIR spectra of biochar from TGA pyrolysis.*

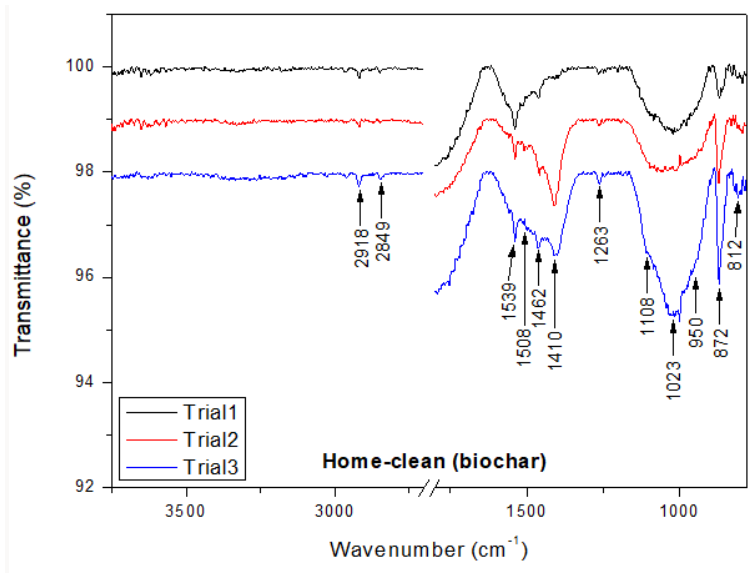

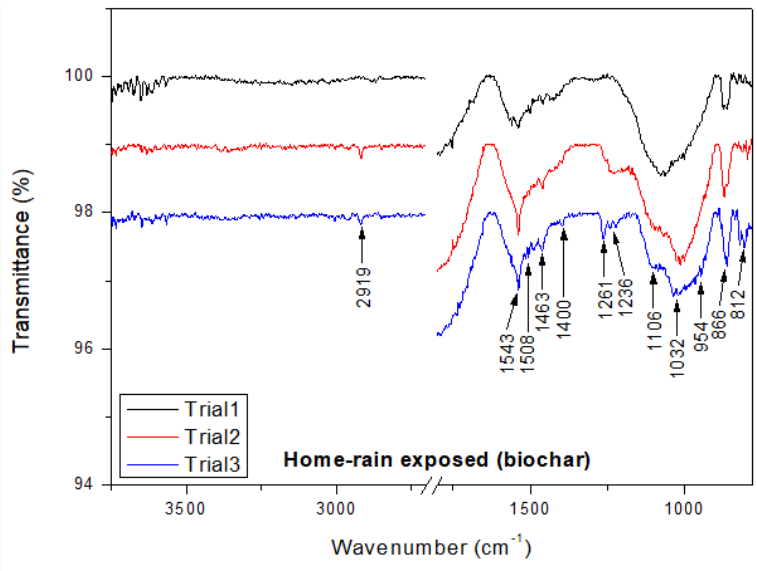

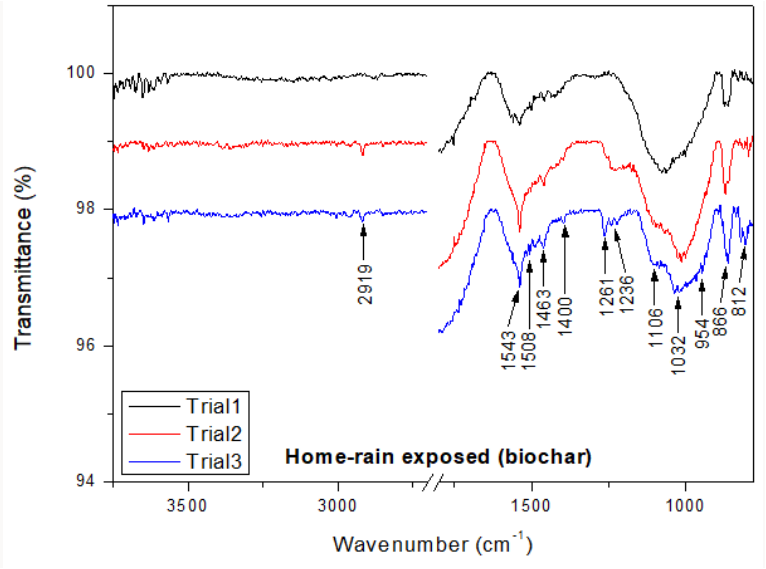

Table 3: *Summary of FTIR characteristic absorption bands of some functional groups in as-received samples and biochar from TGA pyrolysis.*

Assignment	Wavenumber (cm^{-1})					
	As-received			Biochar		
	Home-clean	Home-rain exposed	Industrial-clean	Home-clean	Home-rain exposed	Industrial-clean
ν(O-H)	3334 3289	3334 3289	3334 3290	-	-	-
$\nu_{as}(CH_2)$	2918	2919	2918	2918	2919	2919
ν(C-H)	2850	2851	2850	-	-	-
ν(C=O)	1737	1734	1735	-	-	-
δ(H-O-H)	1648	1651	1643	-	-	-
δ(C=C)	1592 1543 1508	1594 1547 1509	1594 1543 1507	1539 1508	1543 1508	1540 1507
δ scissoring (CH_2), $\delta(CH_3)$	1462 1423	1462 1424	1463 1424	1462 1410	1463 1400	1460
δ(CH), $\delta(CH_3)$	1370	1370	1369	-	-	-
$\gamma(CH_2)$, δ(O-H)	1319	1317	1318	-	-	-
ν(C-O)	1263 1239	1261 1236	1262 1241	1263	1261 1236	1262
ν_{as}(C-O-C)	1156	1156	1156			

ν(C-O), ν(O-H)	1104	1103	1104	1108	1106	1106
ν(C-O)	1051	1050	1050	-	-	-
ν_s(C-O-C)	1027	1026	1026	1023	1032	1021
ν(C-O)				950	954	945
ν(C-C)	898, 812	897, 812	898, 813	872, 812	866, 812	868, 812

Pyrolysis of wood samples release gaseous products. The functional groups of these gaseous products released during the TGA pyrolysis experiments were studied using PerkinElmer Frontier MIR/NIR FTIR spectrometer. FTIR spectra (Figure 7) of functional groups of gaseous products released at different temperatures are shown below. The characteristic FTIR absorption bands of some functional groups and main gaseous products evolved from TGA pyrolysis is given in Table 4. The gaseous products exhibited O-H, C=O, C-C, C-H and C-O functional groups corresponding to different chemical species, such as water, methane, carbon dioxide, carbon monoxide, aldehydes, ketones, acids, alkanes, phenols, ethers and alcohol.

Figure 7: *3D-FTIR spectra of gaseous products evolved from TGA pyrolysis.*

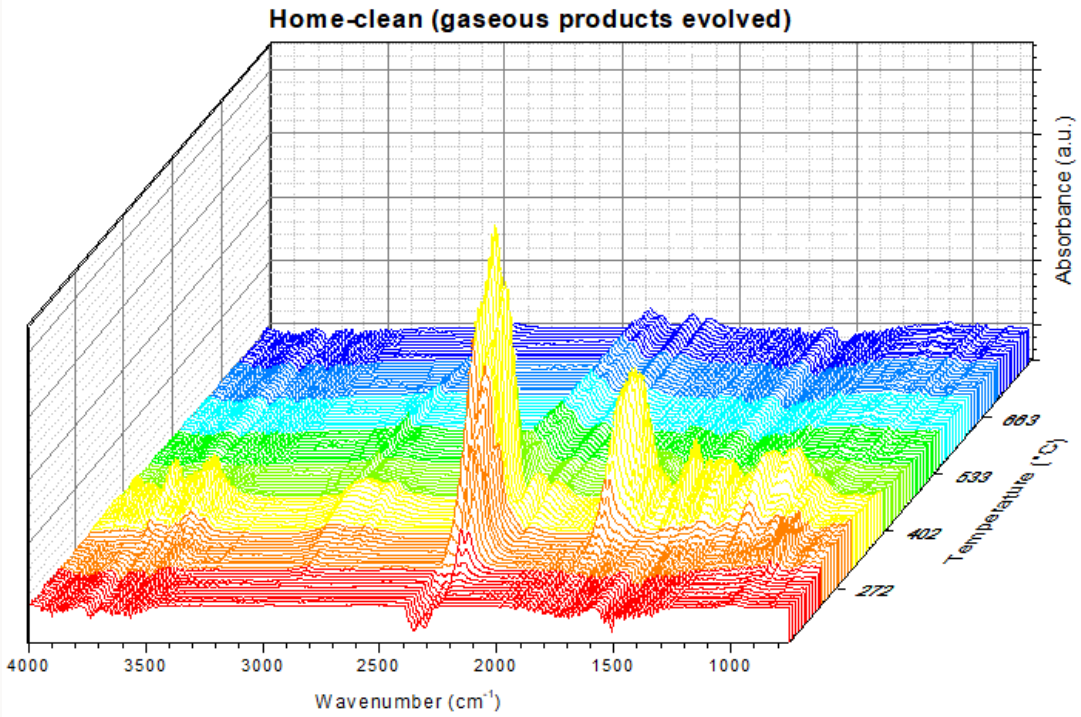

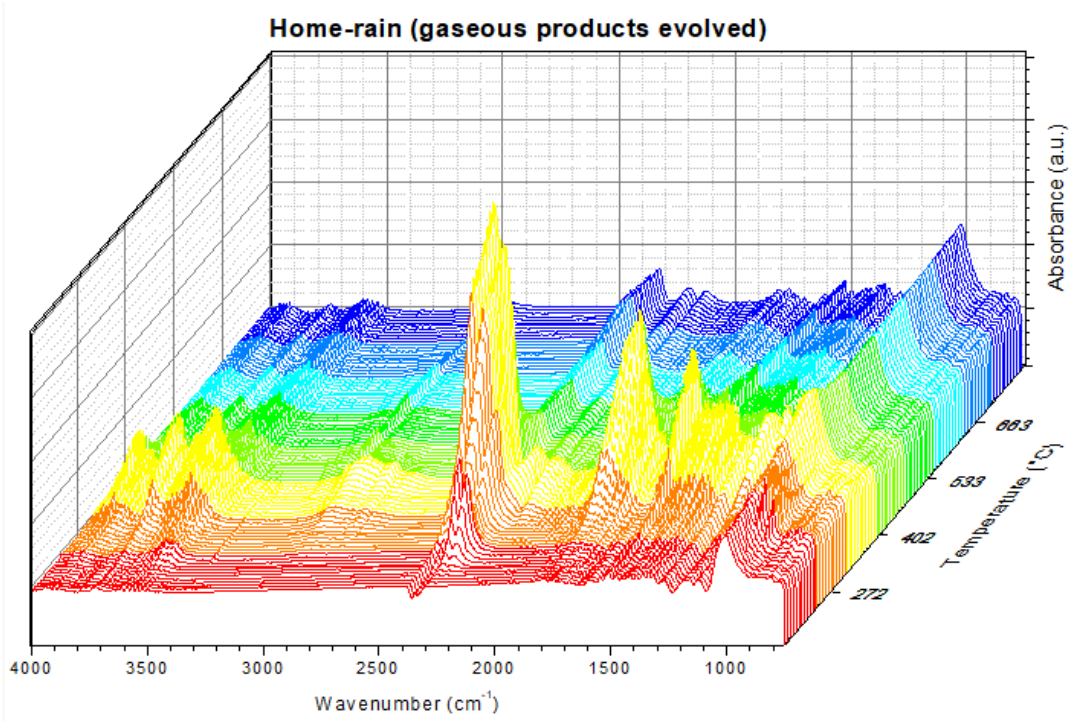
Home-rain (gaseous products evolved)
Absorbance (a.u.)
Temperature (°C)
663
533
402
272
4000
3500
3000
2500
2000
1500
1000
Wavenumber (cm-1)

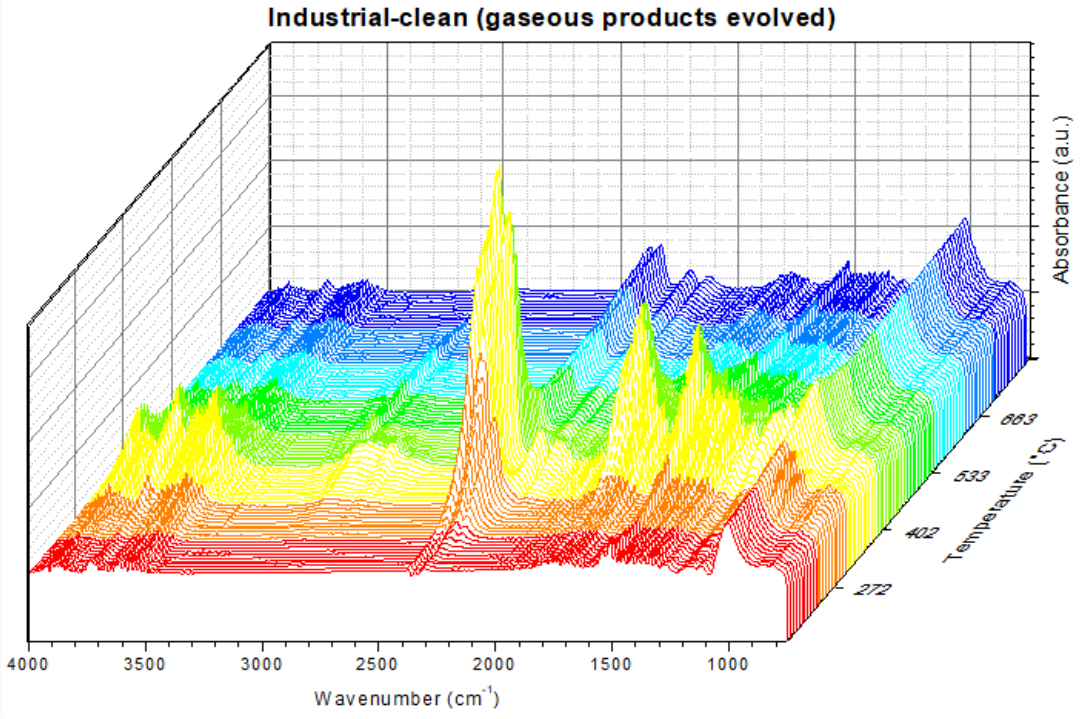
Industrial-clean (gaseous products evolved)
Absorbance (a.u.)
Temperature (°C)
663
533
402
272
4000
3500
3000
2500
2000
1500
1000
Wavenumber (cm-1)

Table 4: *Summary of FTIR characteristic absorption bands of some functional groups and main gaseous products evolved from TGA pyrolysis.*

Assigned species	**Functional group**	**Wavenumber (cm^{-1})**
H_2O	O-H	4000-3000
CH_4	C-H	3000-2700
CO_2	C=O	2400-2250
CO	C-O	2250-2000
Aldehydes, ketones, acids	C=O	1900-1650
Alkanes	C-C, C-H	1460-1365
Phenols	C-O	1300-1200
Ethers	C-O	1275-1060
Alcohol	C-O	1200-1000

The FTIR spectra (Figure 8) of functional groups of gaseous products released at specific thermal degradation temperature of resin, hemicellulose, cellulose and lignin components are also shown below.

Figure 8: *FTIR spectra of gaseous products evolved from TGA pyrolysis compared at degradation peak temperature of resin, hemicelluloses, cellulose and lignin.*

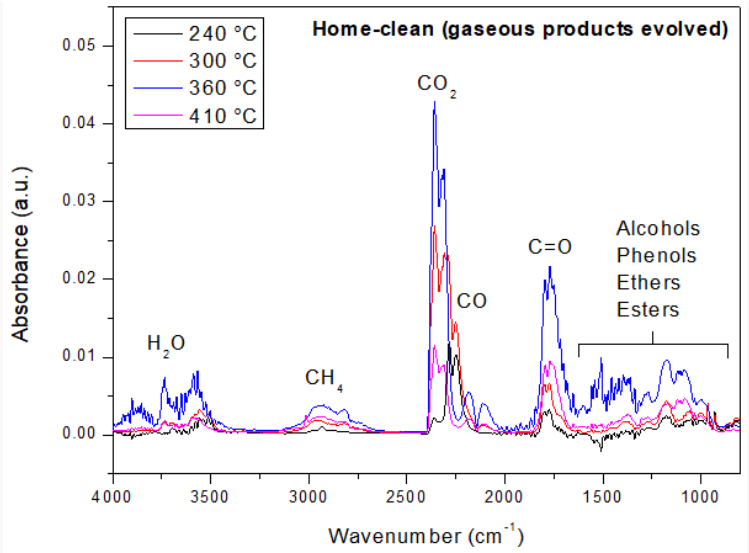

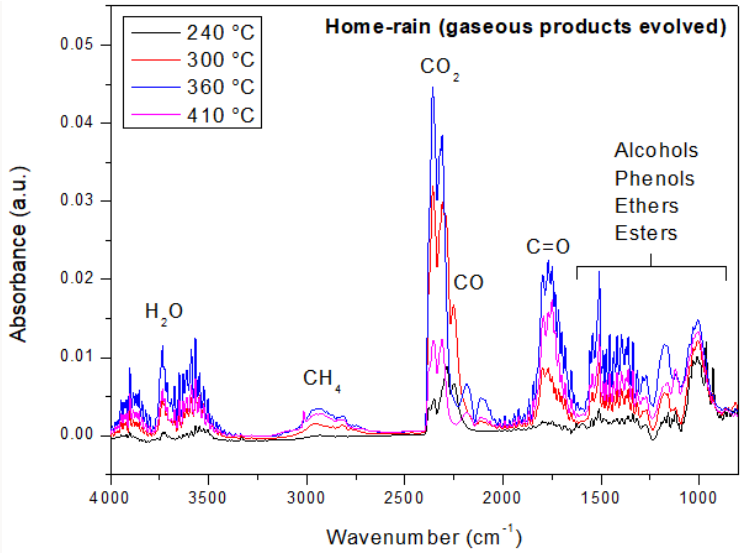

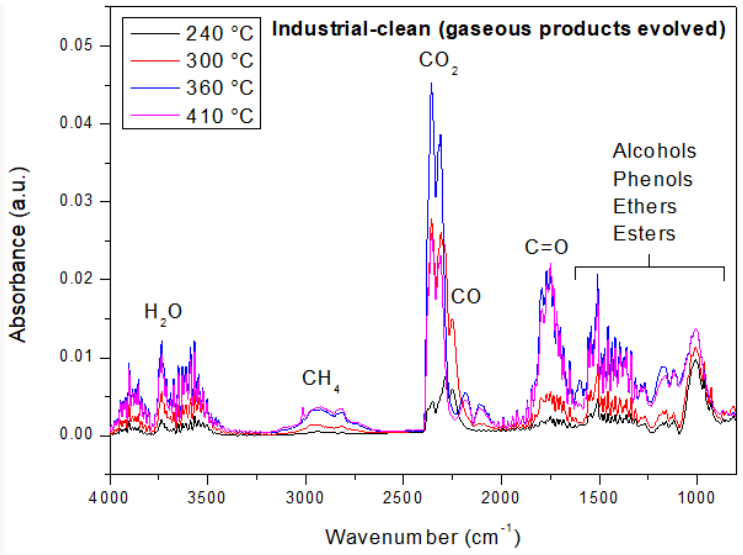

3.3. GC

The gaseous products released during the TGA pyrolysis experiments were studied using PerkinElmer Frontier Clarus 650 GC instrument. GC/MS spectra (Figure 9) of gaseous products released at temperature corresponding to TGA weight loss onset, mid and offset are shown below. The summary of measured retention time of gaseous products at above temperatures and their quantitative match to data library are given in Table 5. The gaseous products analyzed by GC/MS contain both condensable (bio-oil) and non-condensable (syngas) components, which can be separated using a pilot project set-up.

Figure 9: *GC/MS spectra of gaseous products evolved from TGA pyrolysis.*

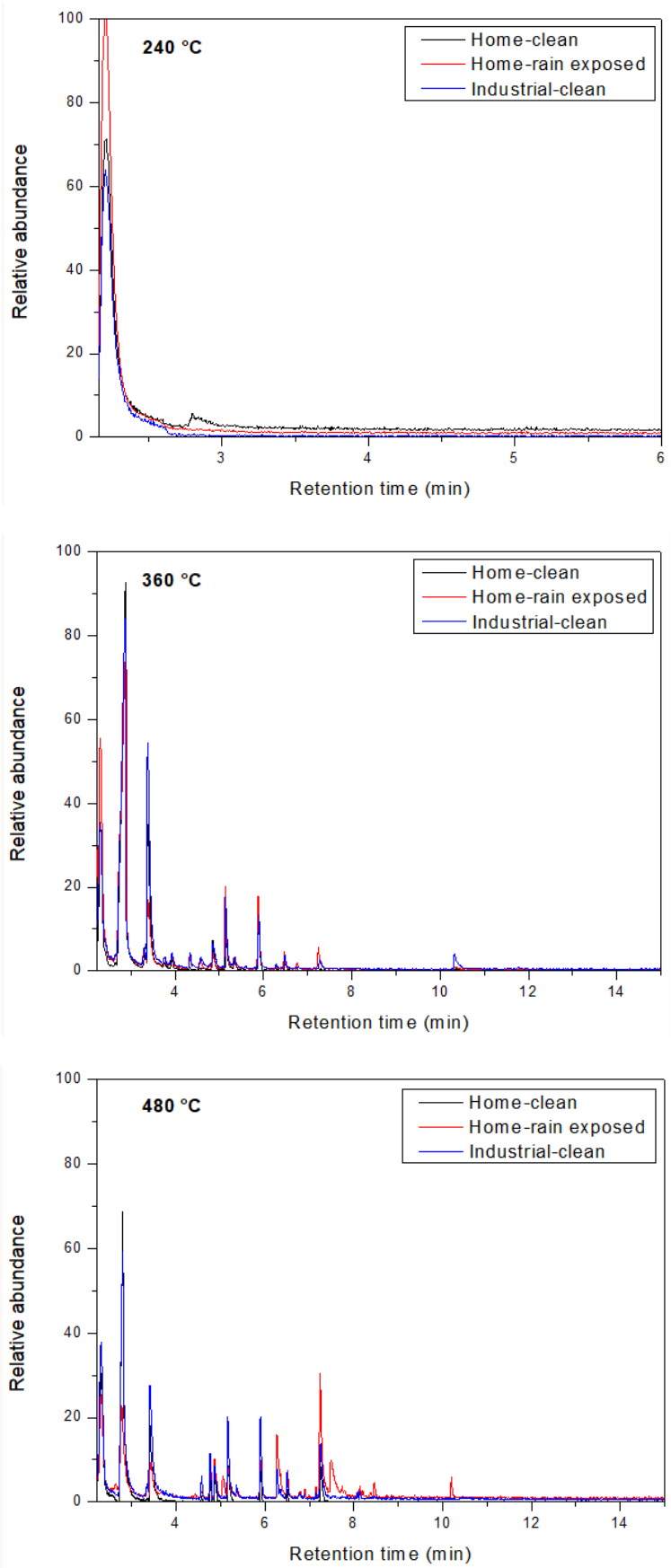

Table 5: *Summary of gaseous products evolved during pyrolysis obtained by TGA-GC/MS.*

Temperature (°C)	**Retention time (min)**	**Library match (%)**	**Name of compound**
240	2.21	43.8	1-Tetrazole-2-yl ethanol
360	2.30	30.5	N-methyl-N'-nitroguanidine
	2.43	27.7	Acetic acid, hydrazide
	2.87	64.3	Ammonium acetate
	3.30	42.7	Methoxyacetonitrile
	3.38	75.0	Acetic acid, hydrazide
	3.76	81.0	Anti-2-Acetoxyacetaldoxime
	3.92	41.2	Acetamide, N-(1-methylpropyl)-
	4.33	36.8	2,3-Dicyano propionamide
	4.56	57.9	Acetamide, 2-cyano-
	4.85	23.3	Propanamide, N-acetyl-
	5.14	31.7	3-Amino-2-oxazolidonone
	5.35	45.8	Carbonocyanidic acid, ethyl ester
	5.89	63.8	3,5-Dimethyl pyrazole-1-methanol
	6.48	52.2	Pyrimidine-2,4(1H,3H)-dione, 5-amino-6-nitroso
	7.28	41.2	1-(1'-Pyrrolidinyl)-2-propanone
	10.34	34.5	3,3-Dimethyl-4-methylamino-butan-2-one
480	2.30	51.3	3-Amino-2-oxazolidonone
	2.79	25.8	Propanoic acid, 2-(aminooxy)
	3.30	31.4	Alanine
	3.40	48.5	Acetic acid, hydrazide
	4.57	52.6	4,5-Dihydroxazole, 2-vinyl-
	4.76	27.4	Benzaldehyde, 4-benzyloxayl-3-methoxy-2-nitro
	4.85	83.4	Pyrimidine-2,4(1H,3H)-dione, 5-amino-6-nitroso
	5.15	52.1	Pyrimidine-2,4(1H,3H)-dione, 5-amino-6-nitroso
	5.36	76.6	Carbonocyanidic acid, ethyl ester

	5.89	33.4	3,5-Dimethyl pyrazole-1-methanol
	6.27	51.2	1H-imidazole-2-methanol
	6.49	39.5	Pyrimidine-2,4(1H,3H)-dione, 5-amino-6-nitroso
	7.25	21.3	1-(1'-pyrrolidinyl)-2-propane
	8.13	61.8	Acetic acid, [(aminocarboxyl)amino]oxo

Fixed-bed pyrolysis experiment (200 ml/min N_2 flow) with 30 g of waste samples each was conducted to analyze the non-condensable gases released during pyrolysis. The qualitative and quantitative information of gases released were measured using Agilent 490 micro-GC instrument. The micro-GC data (Figure 10) of non-condensable gases released during pyrolysis are also shown below. The oven dried (90 °C overnight) waste samples were heated from room temperature (RT) to 800 °C with a heating ramp of 40 °C/min followed by isotherm at 800 °C for 1 hour. The gaseous products released during the pyrolysis were passed through condensers to collect the bio-oil separately, and the non-condensable gases passed through scrubbers (1 M sodium hydroxide and packed silica bed column) to filter pollutants before reaching micro-GC. As the pyrolysis proceeded, increase in concentration of gases, such as carbon dioxide (CO_2), carbon monoxide (CO), methane (CH_4) and hydrogen (H_2) were largely measured. After 1 hour, the concentration of gases was measured to reach zero indicating completion of pyrolysis. The concentration of evolved CO_2, CO, CH_4 and H_2 was measured to reach as high as 30%, 25%, 18% and 23%, respectively during pyrolysis.

Figure 10: *Micro-GC data of gas evolved from fixed-bed pyrolysis after passing through condenser (oil collection) and scrubber (pollutant removal).*

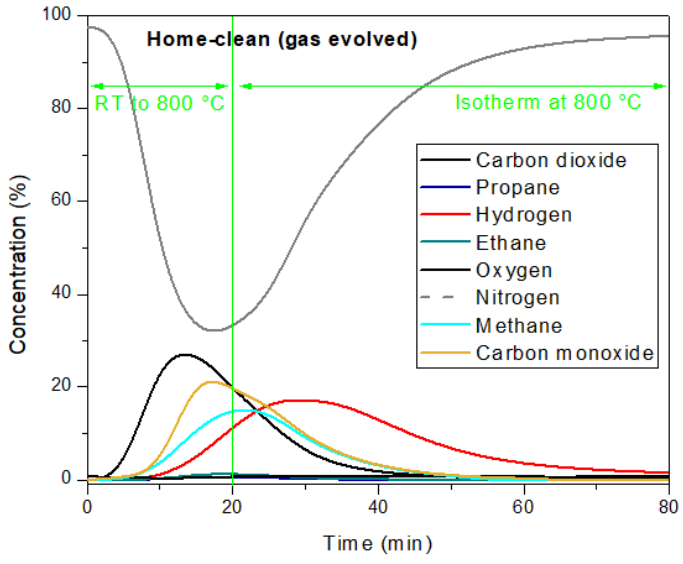

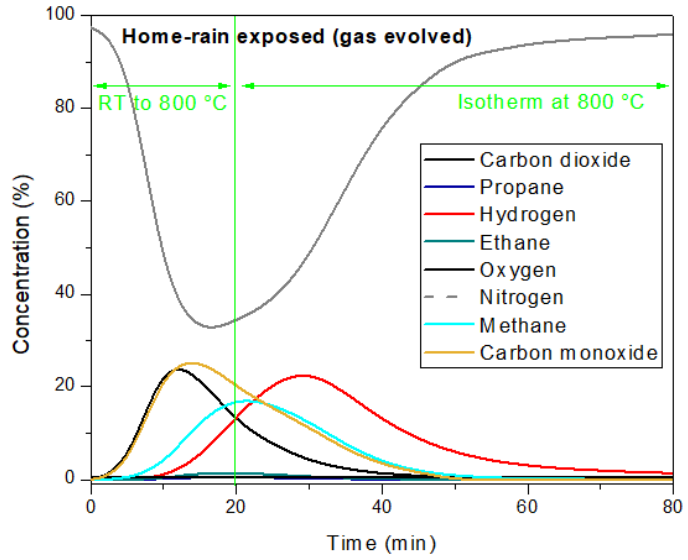

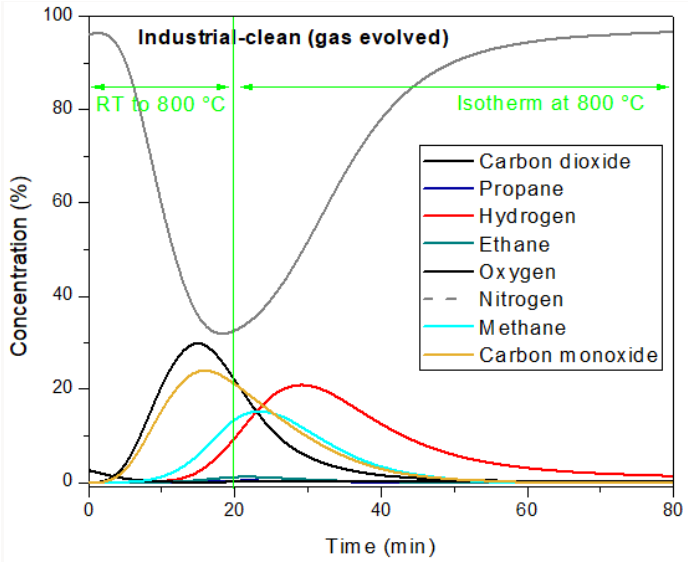

3.4. SEM

The surface morphology, pore structure and shape of biochar from TGA pyrolysis was analyzed using FEI Nova NanoSEM. SEM images of biochars (Figure 11) captured at different magnification are shown below. The HC biochar showed longer and cylindrical cells but with no clearly visible pores on the surface. The HR biochar showed no specific cell structure and no visible pores on the surface. The IC biochar showed longer and cylindrical cells with pores clearly visible on the surface. The IC biochar showed relatively more ordered structure compared to HC and HR biochar.

Figure 11: *SEM images of biochar from TGA pyrolysis.*

Home-clean

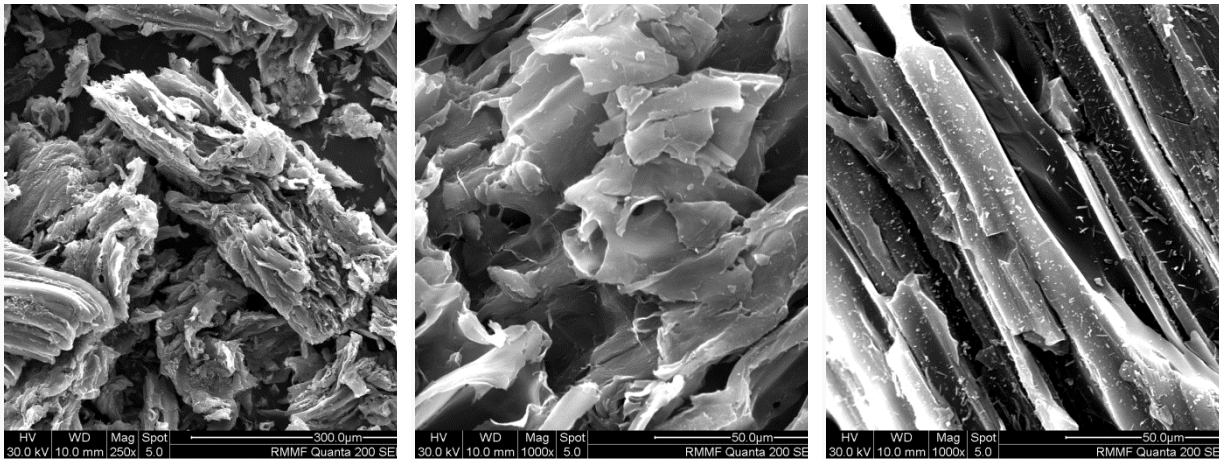

Home-rain exposed

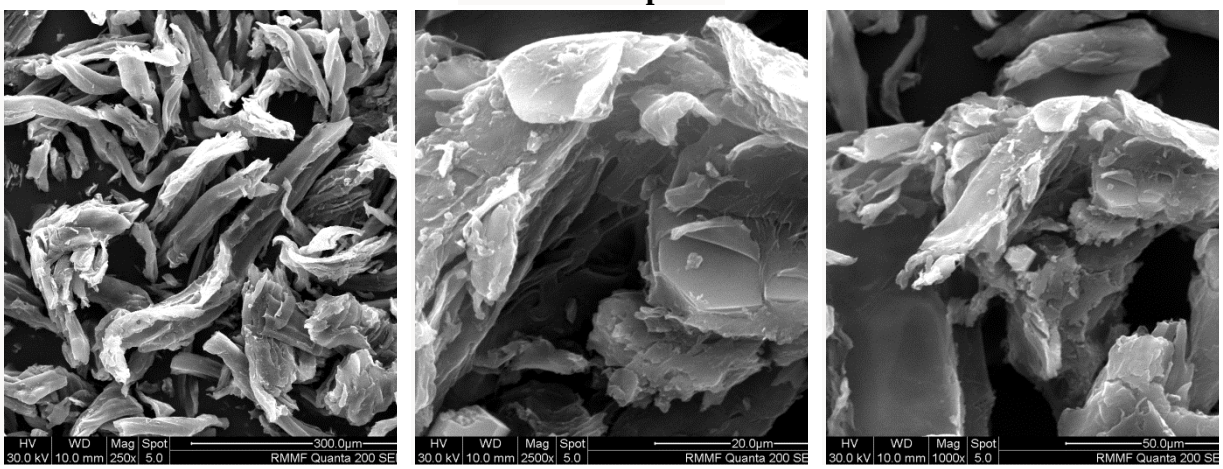

Industrial-clean

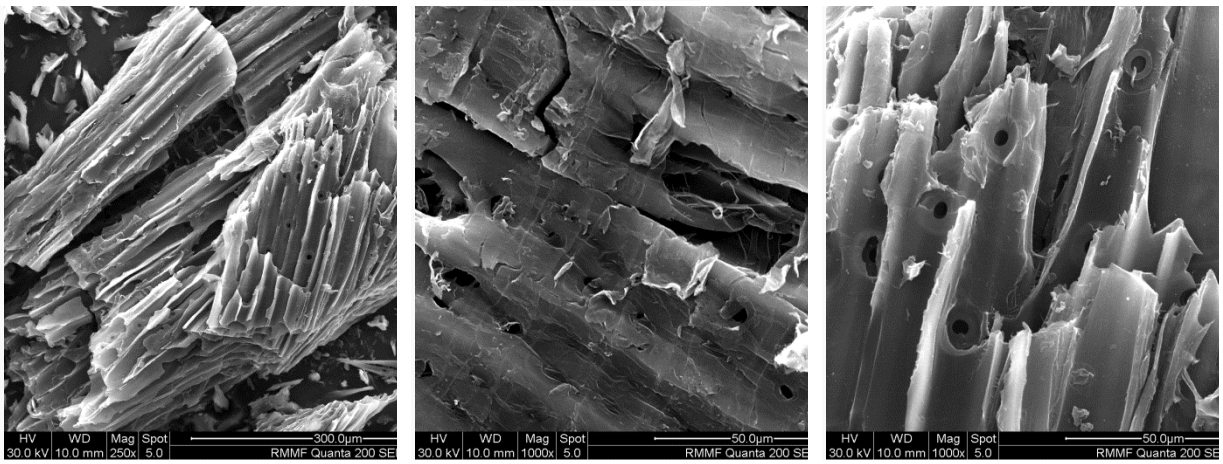

3.5. XRD

The crystalline structure of biochar from TGA pyrolysis was analyzed using Rigaku MiniFlex XRD. XRD pattern of biochars (Figure 12) are shown below. The biochars exhibited broad peaks at 2θ values of 12.1°, 23.4° and 42.9° corresponding to (001), (002) and (100) planes (sp^2 carbon framework) of poorly crystalline turbostratic carbon structure. The biochars also exhibited and sharp peaks at 2θ values of 27.0°, 35.7° and 54.0° corresponding to graphitic structure.

Figure 12: *XRD patterns of biochar from TGA pyrolysis.*

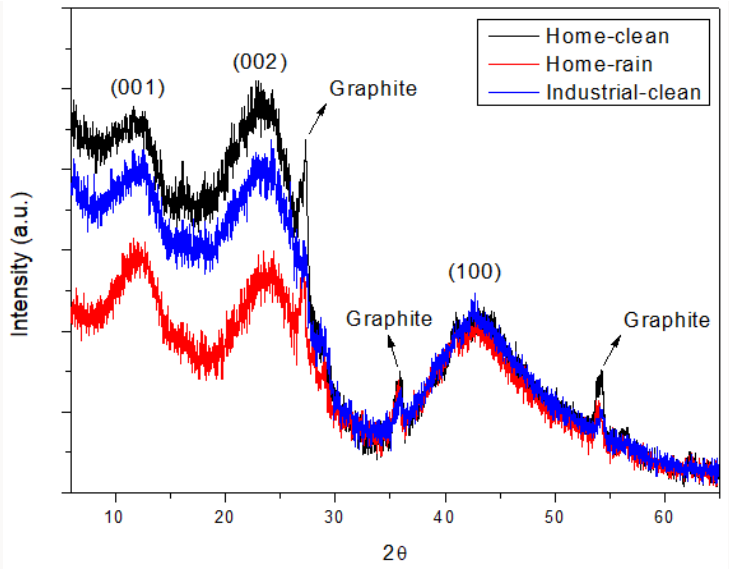

3.6. BET analysis

The surface area and porosity of biochar from TGA pyrolysis was analyzed with the standard N_2 system using Micromeritics Tristar II Plus. The measured surface area and micropore volume of biochars are given in Table 6. In general, the home waste biochars exhibited relatively higher surface area and micropore volume compared to the industry waste biochar.

Table 6: *BET results of biochar from TGA pyrolysis.*

Samples	**Surface area (m^2/g)**	**micropore volume (cm^3/g)**
Home-clean	6.319	0.014
Home-rain exposed	7.440	0.014
Industrial-clean	1.402	0.009

3.7. Elemental analysis

The organic and inorganic elemental composition of as-received waste samples and biochar from TGA pyrolysis was analyzed using PerkinElmer 2400 Series-II CHNS and Nexion 2000B ICP-MS analyzers, respectively. For inorganic elemental analysis, the biochars were digested in 70% nitric acid and diluted to 2% acid for ICP-MS analysis. The measured carbon, hydrogen, nitrogen and sulphur content, and the calculated oxygen oxygen content (determined by difference) are given in Table 7. The carbon and hydrogen content of as-received waste sample was around 50% and 6% respectively, and the nitrogen content of industry sample was relatively higher than home samples. The ICP-MS data (Table 8) showed presence of 14 different inorganic elements in obtained biochars, largely sodium, potassium and calcium. All biochars exhibited high carbon (>90%) and very low inorganic (<0.16%) content. The rain unexposed waste samples exhibited relatively higher nitrogen content (>3.5%) compared to the exposed one. Conversely, the rain exposed home biochar had the highest inorganic content amongst the three tested biochars, which can be attributed to the contribution of inorganic elements generally present in rainwater.

Table 7: *CHNS analysis of as-received samples and biochar from TGA pyrolysis.*

Samples	**C%**	**H%**	**N%**	**S%**	**O%**
Home-clean (as-received)	48.9 ± 1.1	6.2 ± 0.1	4.5 ± 0.1	0.8 ± 0.3	39.6
Home-rain exposed (as-received)	49.1 ± 1.1	6.2 ± 0.4	4.4 ± 0.3	0.7 ± 0.3	39.6
Industrial-clean (as-received)	50.2 ± 1.1	6.5 ± 0.4	5.6 ± 0.2	0.6 ± 0.2	37.1
Home-clean (biochar)	90.3 ± 2.4	1.3 ± 0.2	3.8 ± 0.5	0.5 ± 0.4	4.1
Home-rain exposed (biochar)	94.5 ± 4.1	1.2 ± 0.1	1.5 ± 0.9	0.1 ± 0.1	2.7
Industrial-clean (biochar)	89.2 ± 9.1	1.3 ± 0.1	3.3 ± 0.6	0.1 ± 0.1	6.1

Table 8: *ICP-MS data of biochar from TGA pyrolysis.*

Elements	**mg per kg of biochar**		
	Home-clean	**Home-rain exposed**	**Industrial-clean**
Sodium (Na)	178.738	227.021	185.216
Magnesium (Mg)	35.728	63.666	32.727
Potassium (K)	173.783	288.589	179.101
Calcium (Ca)	305.039	977.221	540.567
Vanadium (V)	0.026	0.041	0.038

Chromium (Cr)	0.107	0.176	0.082
Manganese (Mn)	2.293	5.313	1.891
Iron (Fe)	14.742	14.344	16.527
Cobalt (Co)	6.589	0.190	5.722
Nickel (Ni)	0.254	0.081	0.060
Copper (Cu)	0.912	0.814	0.824
Zinc (Zn)	0.446	1.144	0.374
Arsenic (As)	0.000	0.000	0.000
Silver (Ag)	0.000	0.000	0.000
Cadmium (Cd)	0.014	0.033	0.000
Lead (Pb)	0.001	0.162	0.355
Uranium (U)	0.000	0.000	0.000

4. Conclusions

The Phase 1 study of the project has been completed successfully. The following conclusions are drawn after analysing the experimental results.

- Pyrolysis of the three received timber waste samples produced biochars in the range of 21-24 wt% at 800 °C.
- The as-received home-rain exposed and industry-clean waste samples exhibited relatively high (more than twice) resin and hemicelluloses content compared to home-clean waste sample.
- The obtained biochars contain up to 1.6 wt% ash and 0.16% inorganic elements (largely sodium, magnesium, calcium and iron).
- The biochars exhibited high carbon content (>90 wt%) and very low hydrogen to carbon ratio (<0.015).
- A relatively lower carbon to nitrogen ratio (less than half) was measured for the biochar obtained from rain exposed waste compared to unexposed samples.
- The biochars exhibited poorly crystalline turbostratic sp^2 carbon framework structure with surface area and micropore volume measured in the range of 1.4-7.4 m^2/g and 0.009-0.014 cm^3/g, respectively.
- The biochars clearly demonstrated difference in their morphology, where the industry waste biochar showed visible surface micropores.

- Condensable bio-oil up to 55 wt% and non-condensable gaseous products (largely hydrogen, methane carbon dioxide and carbon monoxide) were released during pyrolysis.

5. Relevant technologies that can be applied for process development

Existing biomass thermal conversion processes to obtain value-added products include combustion (excess O_2), gasification (partial O_2) and pyrolysis (no O_2). While combustion and gasification produce heat and syngas (mixture of H_2, CH_4, C_xH_y, CO_2 and CO) with residue (ash), pyrolysis produces biochar, bio-oil and syngas. From our in-lab fixed-bed pyrolysis test it is evident that fuel gases, such as H_2 (up to 23%) and CH_4 (up to 18%) are produced during pyrolysis of waste samples provided by ISJO. The syngas obtained from pyrolysis of such samples can be used as fuel for generation of heat and power using combustion engine technology [3]. For commercial applications, pure H_2 and CH_4 can also be separated from the obtained syngas using technologies, such as a regenerative system [4], membrane separation [5], etc. The bio-oil (up to 55 wt%) obtained from pyrolysis can also be used as an alternative renewable fuel source to produce hydrogen by industry adaptable technologies, such as steam reforming, oxidative steam reforming, aqueous phase reforming and partial oxidation [6]. Moreover, co-pyrolysis using plastic or tyre waste can also be performed as an optional technique to obtain high-grade pyrolysis oil [7]. Customized pilot prototype for production of biochar from pyrolysis of wood waste, along with storage or utilization of bio-oil and syngas derivative is also possible via large firms like Earth Systems (https://www.esenergy.com.au/) and Pyrotech Energy (https://pyrotechenergy.com/).

6. Market analysis and future recommendations for Phase 2 study

Based on the market analysis and the quality of the obtained biochars, the following applications are recommended for Phase 2. Upon further feedback from ISJO, we can restrict the focus to specific application and product development in Phase 2 that are of interest to ISJO. If required, further experiments can be performed on this showcasing RMIT proof-of-concepts as well, highlighting any advantages.

6.1. Hydrogen storage material

The biochars can be used as potential hydrogen physical adsorption materials (as an alternative to conventional activated carbon), where the sodium or potassium inorganic elements present in biochars could provide stabilization to adsorbed molecular hydrogen [8]. Moreover, the pore

structure of biochar and surface functional groups can also be tuned via chemical (e.g. potassium hydroxide, zinc or magnesium chloride) or steam/carbon dioxide activation for increased hydrogen adsorption capacity [9].

6.2. Fuel for direct carbon fuel cells (DCFCs)

The biochars can be used as promising carbonaceous solid fuel for generation of electricity using DCFCs in molten carbonate fuel systems, where the power output can also be further improved using metal oxides as catalyst for carbon oxidation [10]. Moreover, the presence of inorganic elements, such as potassium and calcium in biochar could remarkably lower the carbon fuel gasification temperature and improve power density output at relatively low temperatures [11].

6.3. Electrode material for supercapacitor

The biochars can be used as promising support material for growth of the carbon nanofibers, which can be directly used as electrode material for double-layer electrochemical capacitors [12]. The specific surface area of biochars can be improved by decreasing the particle size using physical strategies like ball milling. The as prepared biochar may also exhibit pseudocapacitance arising from the redox reactions of the residue nitrogen and oxygen functionalities [13].

6.4. Adsorbent for water treatment

The biochars can be used as promising adsorbent material for elimination of wide range of pollutants, such as heavy metal ions, organics, antibiotics, etc., where the adsorption mechanism depends on the adsorbent–adsorbate interactions, such as electrostatic attraction, p–p bond interaction, H-bonding, hydrophobic interactions, ion exchange and pore-filling [14]. The adsorbent efficiency of the system can also be improved by using biochar as support material for generating nanoscale zero-valent iron, which has high affinity for heavy metal pollutants [15].

6.5. Additive for construction materials

The biochars can be used as promising additive material in fabricating cement-based composites to improve strength, reduce curing time and carbon footprint, where carbon dioxide curing can accelerate carbonation more effectively than air curing, thereby promoting recycling and carbon dioxide utilization [16]. The biochars can also be used as promising additive material in fabricating recycled polymer-based composites to improve dynamic modulus,

dimensional stability, and thermal stability in an oxidative environment, and also their 3D printability [17].

6.6. Pigment for flexographic inks

The biochars can be used as promising ink pigment replacing carbon black, where the quality of the ink can be improved by wet milling biochar to 1-5 micron size particles, followed by purification and formulation of flexographic conducting inks comprising polymer binders, solvents and additives [18]. Moreover, the viscoelastic properties of the inks can also be tuned for extrusion printing flexible electrical circuits.

8. References

[1] L. Pan, Y. Jiang, L. Wang, W. Xu, Kinetic Study on the Pyrolysis of Medium Density Fiberboard: Effects of Secondary Charring Reactions, Energies 11(9) (2018).
[2] V. Emmanuel, B. Odile, R. Céline, FTIR spectroscopy of woods: A new approach to study the weathering of the carving face of a sculpture, Spectrochimica Acta Part A: Molecular and Biomolecular Spectroscopy 136 (2015) 1255-1259.
[3] F.Y. Hagos, A.R.A. Aziz, S.A. Sulaiman, Trends of Syngas as a Fuel in Internal Combustion Engines, Advances in Mechanical Engineering 6 (2014) 401587.
[4] A. Campen, K. Mondal, T. Wiltowski, Separation of hydrogen from syngas using a regenerative system, International Journal of Hydrogen Energy 33(1) (2008) 332-339.
[5] A. Kertik, L.H. Wee, M. Pfannmöller, S. Bals, J.A. Martens, I.F.J. Vankelecom, Highly selective gas separation membrane using in situ amorphised metal–organic frameworks, Energy & Environmental Science 10(11) (2017) 2342-2351.
[6] A. Kumar, J.P. Chakraborty, R. Singh, Bio-oil: the future of hydrogen generation, Biofuels 8(6) (2017) 663-674.
[7] F. Abnisa, W.M.A. Wan Daud, A review on co-pyrolysis of biomass: An optional technique to obtain a high-grade pyrolysis oil, Energy Conversion and Management 87 (2014) 71-85.
[8] R. Ströbel, J. Garche, P.T. Moseley, L. Jörissen, G. Wolf, Hydrogen storage by carbon materials, Journal of Power Sources 159(2) (2006) 781-801.
[9] W.-J. Liu, H. Jiang, H.-Q. Yu, Development of Biochar-Based Functional Materials: Toward a Sustainable Platform Carbon Material, Chemical Reviews 115(22) (2015) 12251-12285.
[10] A. Kacprzak, R. Kobyłecki, R. Włodarczyk, Z. Bis, The effect of fuel type on the performance of a direct carbon fuel cell with molten alkaline electrolyte, Journal of Power Sources 255 (2014) 179-186.
[11] S.Y. Ahn, S.Y. Eom, Y.H. Rhie, Y.M. Sung, C.E. Moon, G.M. Choi, D.J. Kim, Utilization of wood biomass char in a direct carbon fuel cell (DCFC) system, Applied Energy 105 (2013) 207-216.
[12] W.-J. Liu, K. Tian, Y.-R. He, H. Jiang, H.-Q. Yu, High-Yield Harvest of Nanofibers/Mesoporous Carbon Composite by Pyrolysis of Waste Biomass and Its Application for High Durability Electrochemical Energy Storage, Environmental Science & Technology 48(23) (2014) 13951-13959.
[13] D. Hulicova-Jurcakova, M. Seredych, G.Q. Lu, T.J. Bandosz, Combined Effect of Nitrogen- and Oxygen-Containing Functional Groups of Microporous Activated Carbon on its Electrochemical Performance in Supercapacitors, Advanced Functional Materials 19(3) (2009) 438-447.

[14] Y. Liu, W. Zheng, S. You, Chapter 15 Engineering Biochars for Environmental Applications, Emerging Nanotechnologies for Water Treatment, The Royal Society of Chemistry2022, pp. 426-446.
[15] D. Yang, L. Wang, Z. Li, X. Tang, M. He, S. Yang, X. Liu, J. Xu, Simultaneous adsorption of Cd(II)andAs(III)by a novel biochar-supported nanoscale zero-valent iron in aqueous systems, Science of The Total Environment 708 (2020) 134823.
[16] L. Wang, L. Chen, D.C.W. Tsang, B. Guo, J. Yang, Z. Shen, D. Hou, Y.S. Ok, C.S. Poon, Biochar as green additives in cement-based composites with carbon dioxide curing, Journal of Cleaner Production 258 (2020) 120678.
[17] M. Idrees, S. Jeelani, V. Rangari, Three-Dimensional-Printed Sustainable Biochar-Recycled PET Composites, ACS Sustainable Chemistry & Engineering 6(11) (2018) 13940-13948.
[18] Y. Goh, S. Lauro, S.T. Barber, S.A. Williams, T.A. Trabold, Cleaner production of flexographic ink by substituting carbon black with biochar, Journal of Cleaner Production 324 (2021) 129262.